

This talk will be presented at LWS Geostorm CDAW and Conference on 5-9 March 2007 - Florida Tech - Melbourne, FL

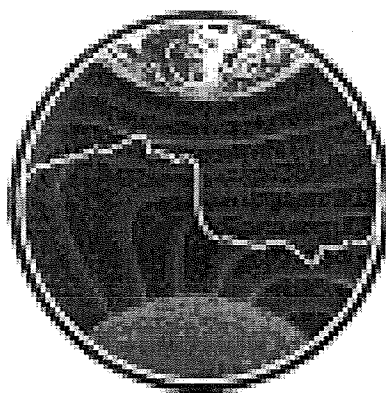
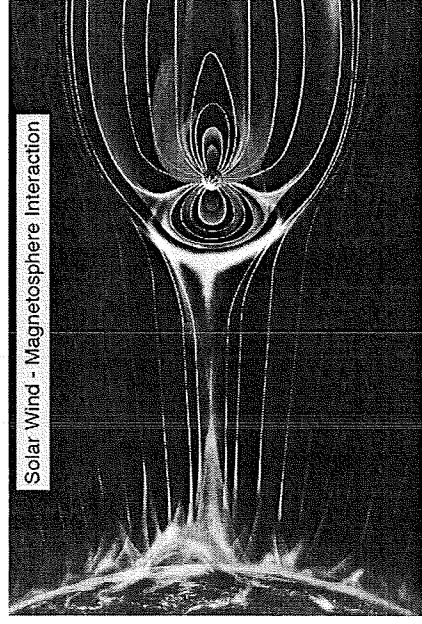
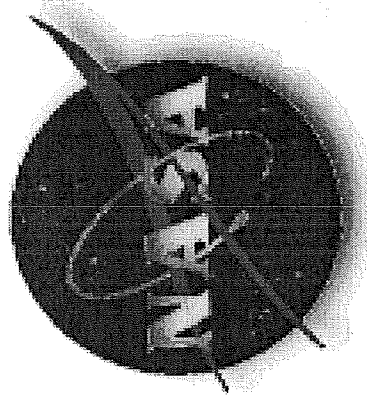
Effect of EMIC Wave Normal Angle Distribution on Relativistic Electron Scattering Based on the Newly Developed Self-Consistent RC/EMIC Waves Model by Khazanov et al. [2006]

Khazanov, G.V., D. L. Gallagher, and K. Gamayunov

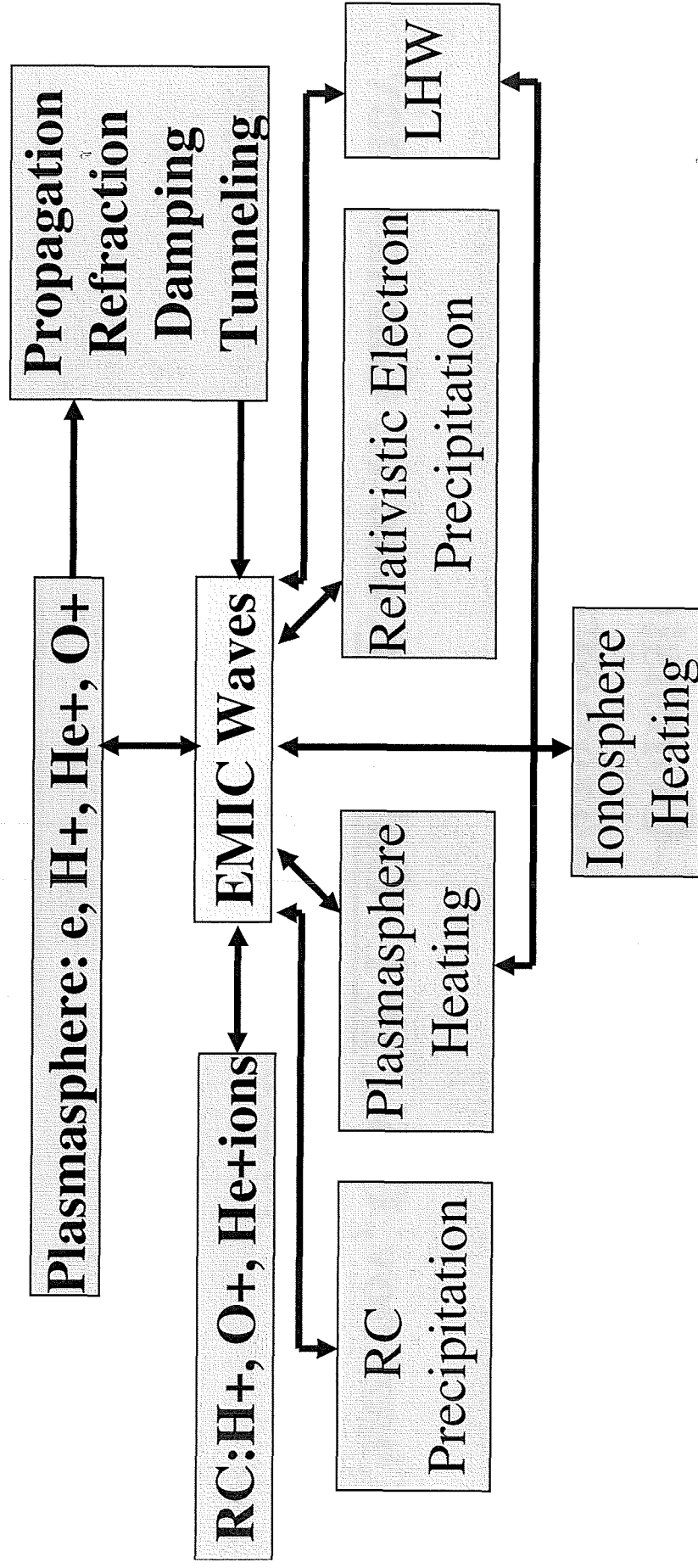
It is well known that the effects of EMIC waves on RC ion and RB electron dynamics strongly depend on such particle/wave characteristics as the phase-space distribution function, frequency, wave-normal angle, wave energy, and the form of wave spectral energy density. Therefore, realistic characteristics of EMIC waves should be properly determined by modeling the RC-EMIC waves evolution self-consistently. Such a self-consistent model progressively has been developing by *Khazanov et al.* [2002-2006]. It solves a system of two coupled kinetic equations: one equation describes the RC ion dynamics and another equation describes the energy density evolution of EMIC waves. Using this model, we present the effectiveness of relativistic electron scattering and compare our results with previous work in this area of research

Effect of EMIC Wave Normal Angle Distribution on Relativistic Electron Scattering Based on the Newly Developed Self-Consistent RC/EMIC Waves Model by Khazanov et al. [2006]

Khazanov, G.V., D. L. Gallagher, and K. Gamayunov
NASA/MSFC/VP62, Huntsville, Alabama, USA



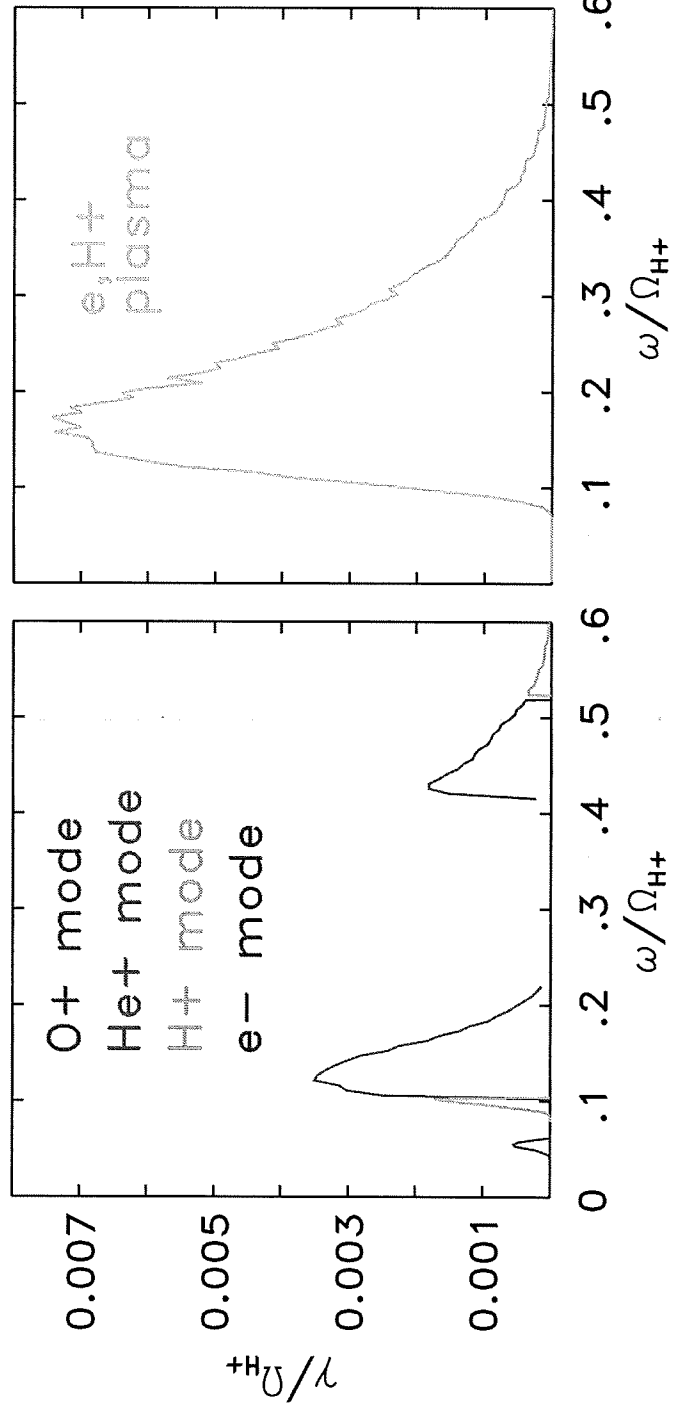
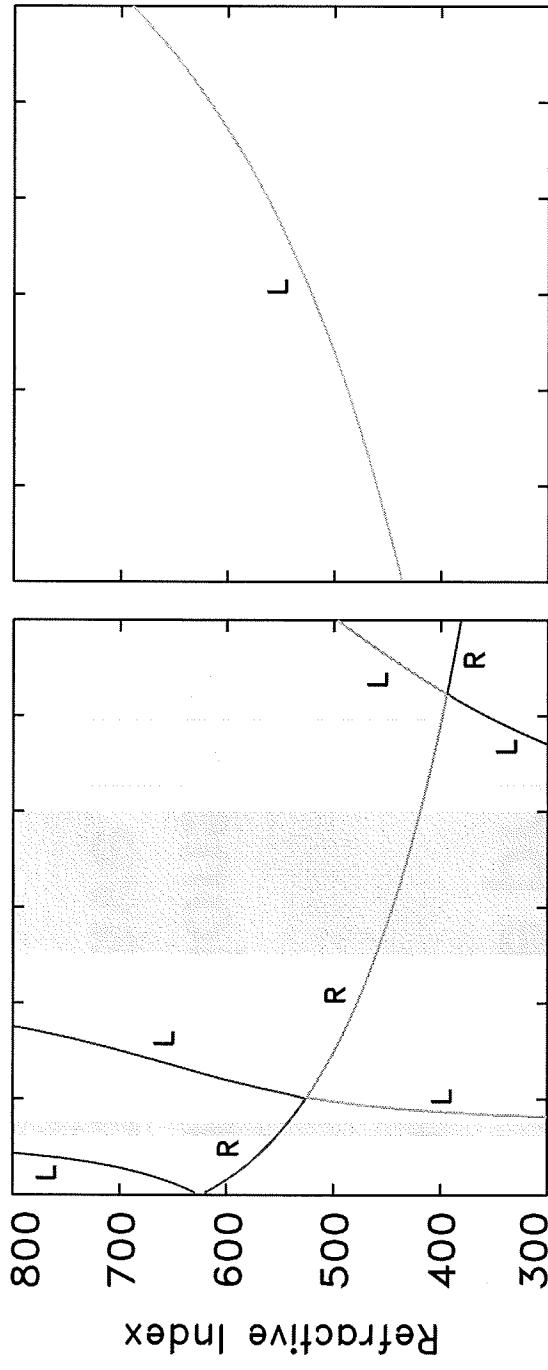
EMIC Waves-RC-Plasmasphere-Ionosphere Coupling



New RC/EMIC Waves Modeling Features

- **Explicit SC solutions for RC PD and EMIC wave PSD**
- **Explicit wave propagation/refraction modeling**
- **No assumptions regarding the shapes of PD and wave PSD**

Refractive Indices and Growth Rates



RC Model with WPI

- Particles

$$\frac{\partial Q}{\partial t} + \frac{1}{R_o^2} \frac{\partial}{\partial R_o} \left(R_o^2 \left\langle \frac{dR_o}{dt} \right\rangle Q \right) + \frac{\partial}{\partial \varphi} \left(\left\langle \frac{d\varphi}{dt} \right\rangle Q \right) + \frac{1}{\sqrt{E}} \frac{\partial}{\partial E} \left(\sqrt{E} \left\langle \frac{dE}{dt} \right\rangle Q \right) + \frac{1}{f(\mu_o)\mu_o} \frac{\partial}{\partial \mu_o} \left(f(\mu_o)\mu_o \left\langle \frac{d\mu_o}{dt} \right\rangle Q \right) = \left\langle \frac{\delta Q}{\delta t} \right\rangle_{collis}$$

- EMIC Waves

$$\frac{\partial^2 (t, r_0, \varphi, \omega, \theta_0)}{\partial t} + \langle \dot{r}_0 \rangle \cdot \frac{\partial^2}{\partial \dot{r}_0} + \langle \dot{\theta}_0 \rangle \cdot \frac{\partial^2}{\partial \theta_0} = 2 \langle \chi(t, r_0, \varphi, \omega, \theta_0) \rangle \cdot B^2$$

$$\frac{d\mathbf{r}}{dt} = \frac{\partial \omega}{\partial \mathbf{k}} = \mathbf{v}_g; \quad \frac{d\mathbf{k}}{dt} = - \frac{\partial \omega}{\partial \mathbf{r}}.$$

RAM with WPI

- Particles

$$\frac{\partial Q}{\partial t} + \frac{1}{R_o^2} \frac{\partial}{\partial R_o} \left(R_o^2 \left\langle \frac{dR_o}{dt} \right\rangle Q \right) + \frac{\partial}{\partial \varphi} \left(\left\langle \frac{d\varphi}{dt} \right\rangle Q \right) + \frac{1}{\sqrt{E}} \frac{\partial}{\partial E} \left(\sqrt{E} \left\langle \frac{dE}{dt} \right\rangle Q \right) + \frac{1}{f(\mu_o) \mu_o} \frac{\partial}{\partial \mu_o} \left(f(\mu_o) \mu_o \left\langle \frac{d\mu_o}{dt} \right\rangle Q \right) = \left\langle \frac{\delta Q}{\delta t} \right\rangle_{collis}$$

- EMIC Waves in RAM code

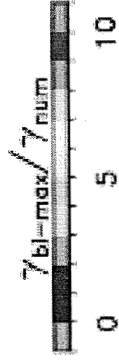
$$B_w = B_{sat} \frac{(G - G_{max})}{G_{min}};$$

G_{min} and G_{max} are 20 and 60 dB; 0.1 – 10 nT range for B_w was adapted.

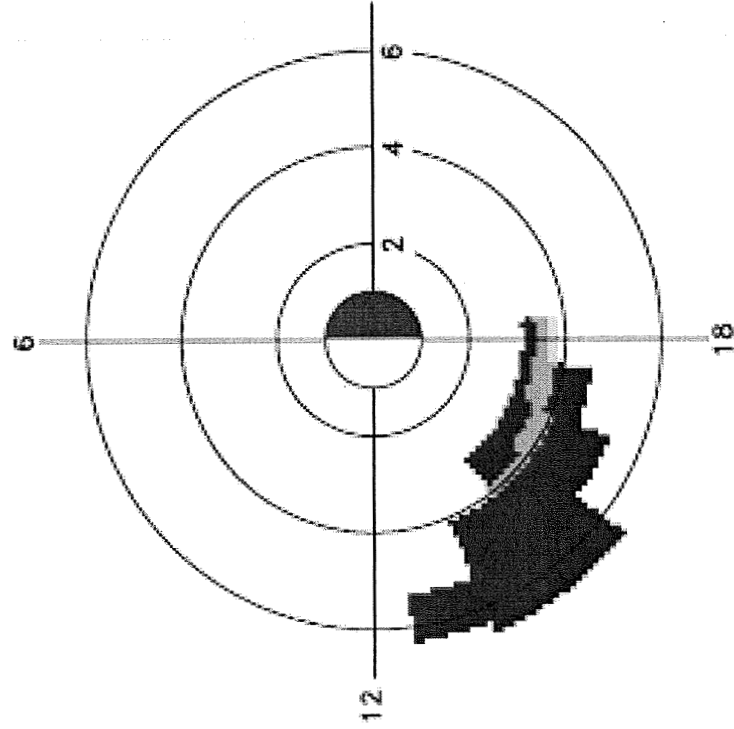
Bi-Maxwellian DF versus Numerical

May 1-7, 1998 Magnetic Storm, Hour 48

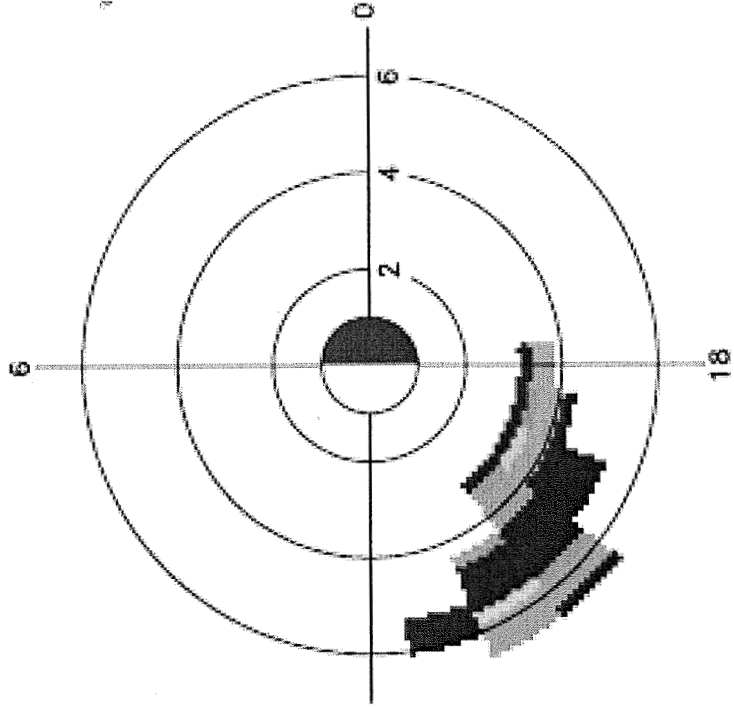
Ratio of Bi-Maxwellian Gamma to Numerical Gamma



No waves

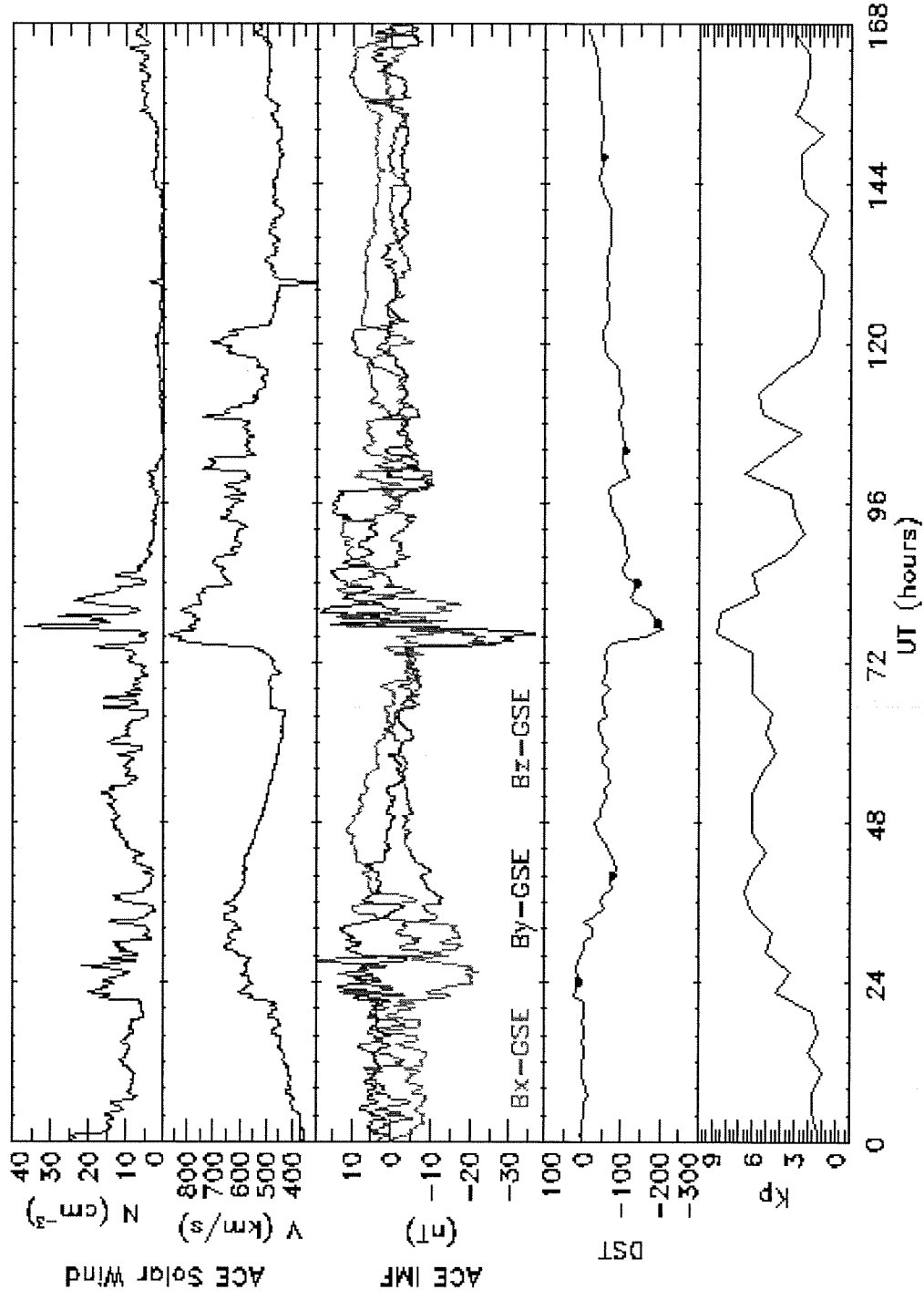


RAM

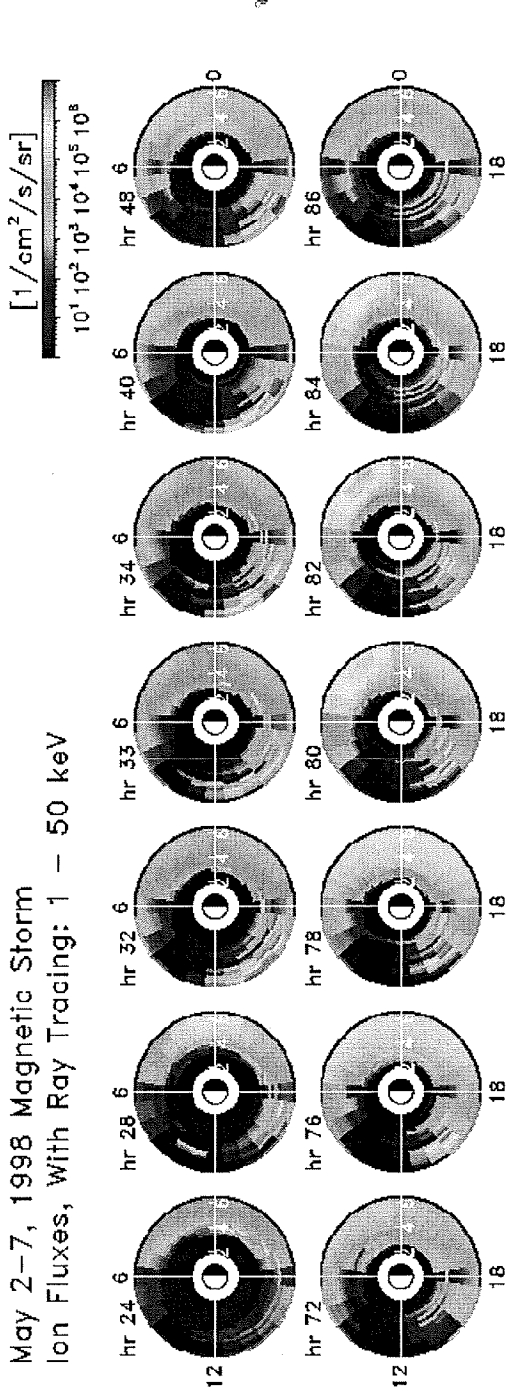
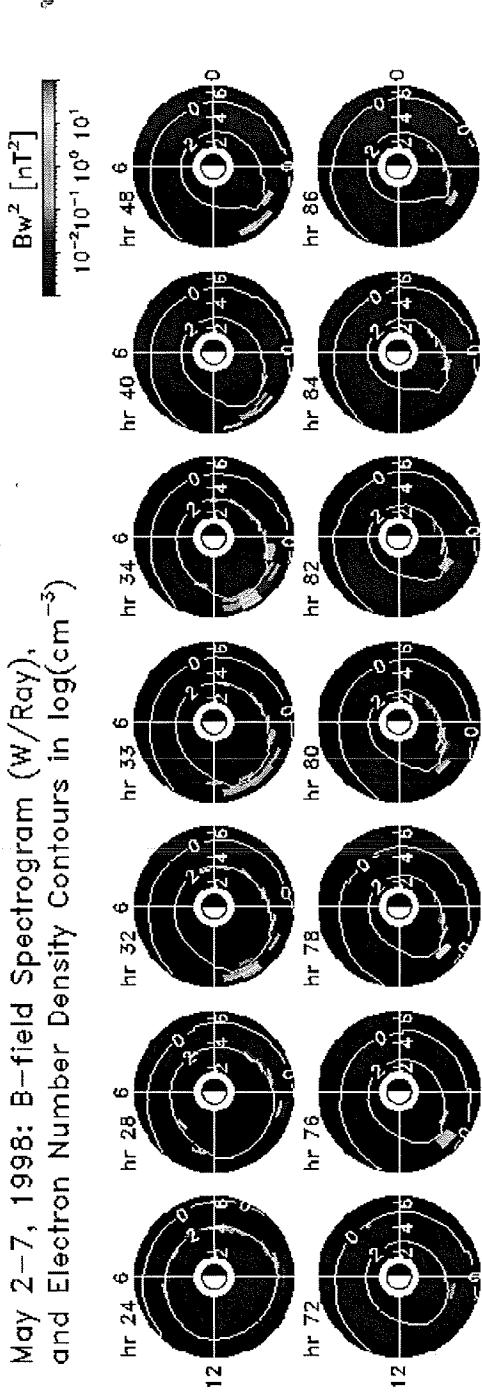


Storm History

May 1-7, 1998 Magnetic Storm



EMIC Waves and RC Precipitations

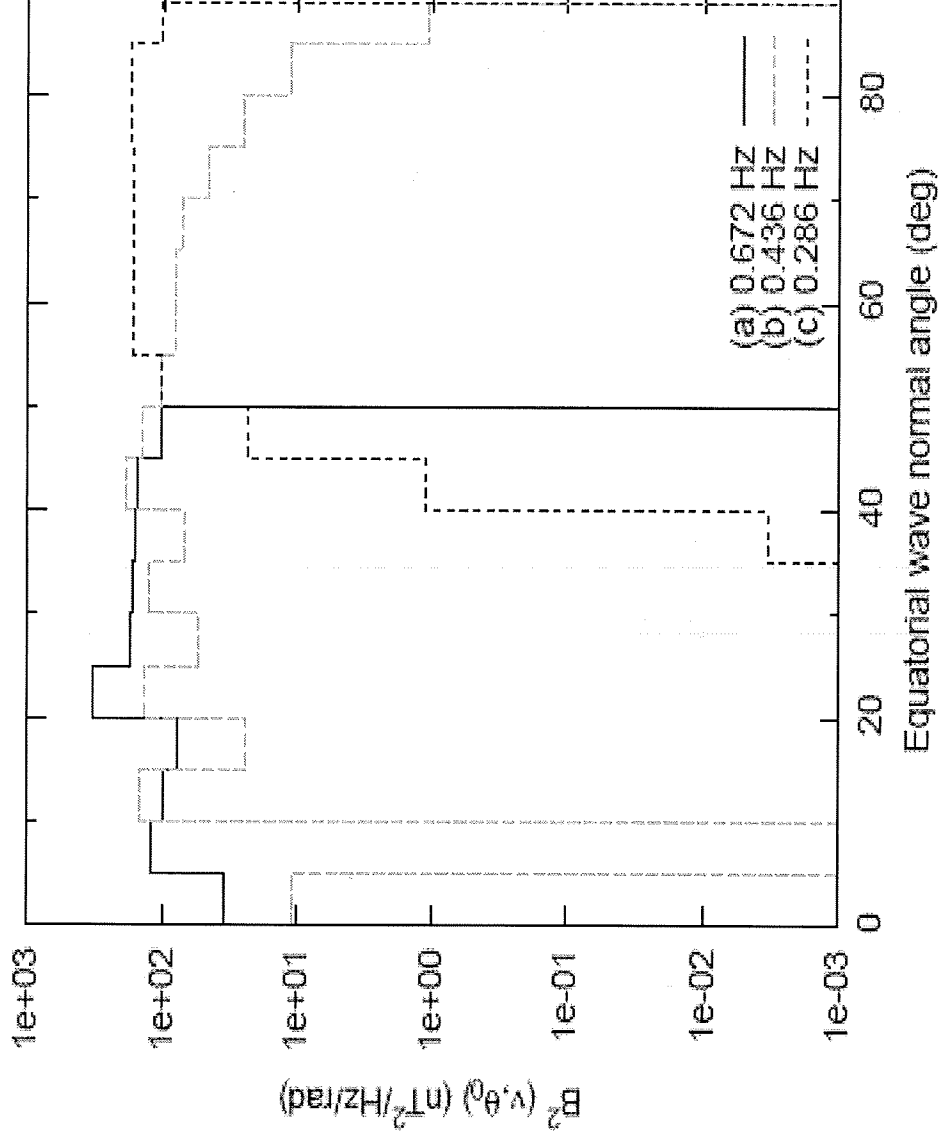


Most intense precipitations are not necessary related to the most intense waves

$UT = 48, MLT = 14, B^2 = 16.3\gamma^2, F = 1.4 \cdot 10^5 (\text{cm}^2 \text{ster})^{-1}$

$UT = 86, MLT = 16, B^2 = 2.7\gamma^2, F = 3.5 \cdot 10^6 (\text{cm}^2 \text{ster})^{-1}$

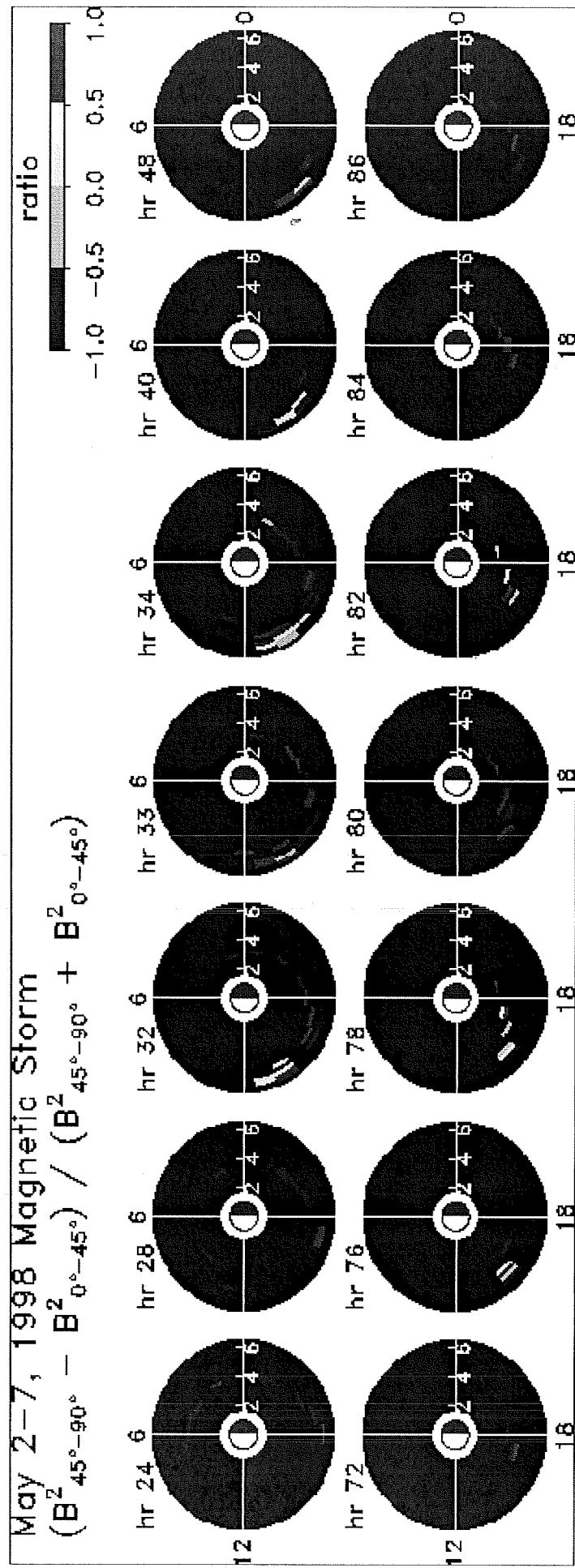
Equatorial PSD for He+-mode EMIC Waves



All the squared magnetic field spectra are obtained at 48 hours after 0000 UT on 1 May, 1998. (a) $L=5.25$, $MLT=16$, (b) $L=5.75$, $MLT=15$, and (c) $L=5.75$, $MLT=14$ [Khazanov *et al.*, 2006].

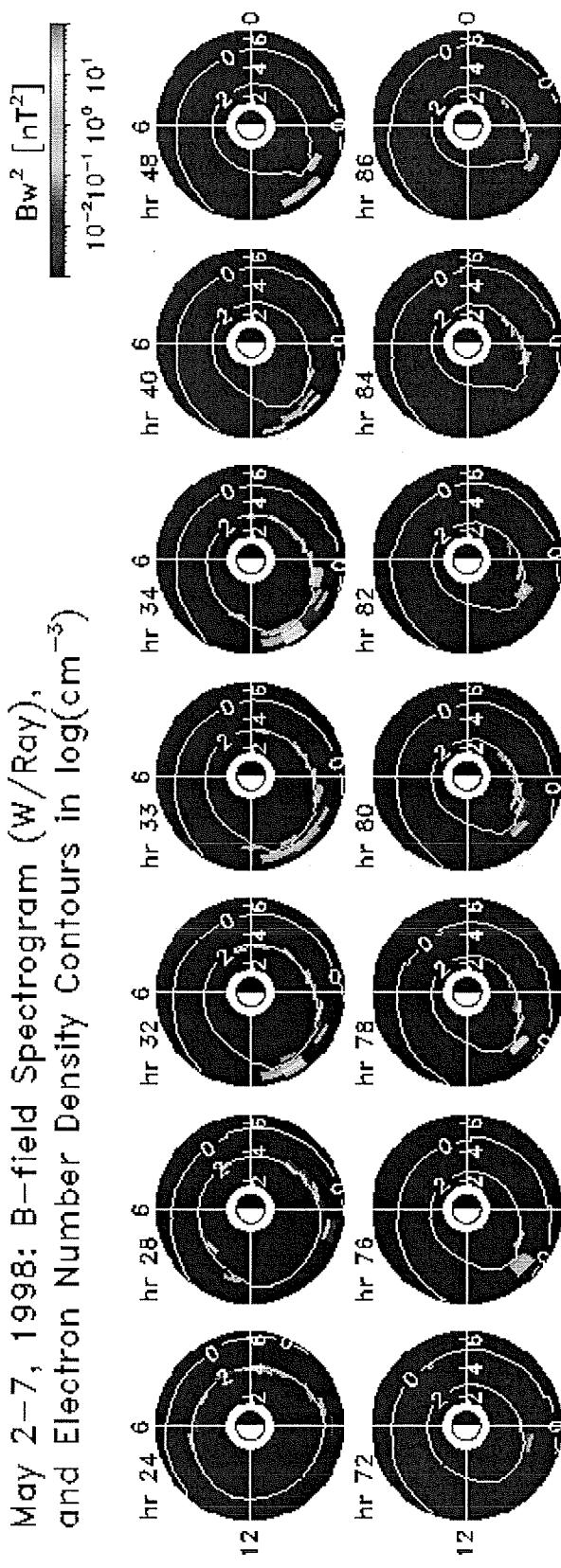
Only one model is capable to do this job. Convective growth rate is incapable to do this.

The Global View of the Wave Distribution Anisotropy

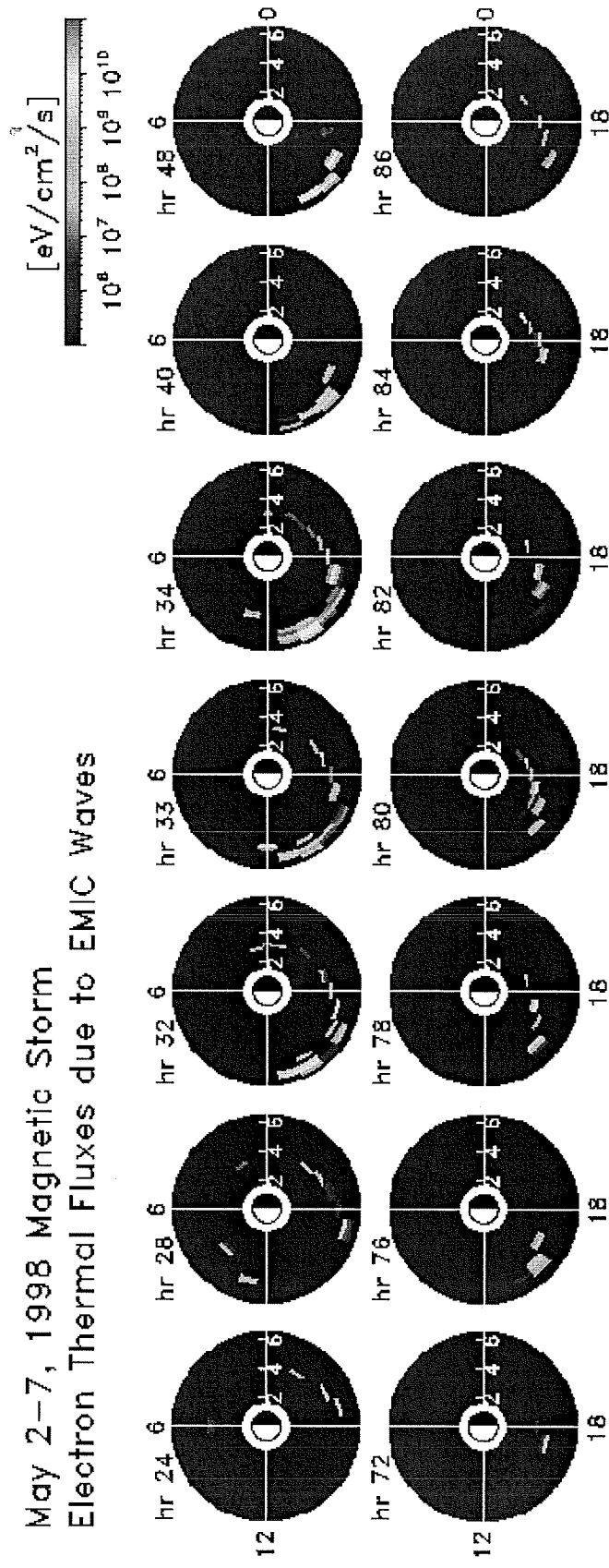


EMIC Waves and Electron Heating

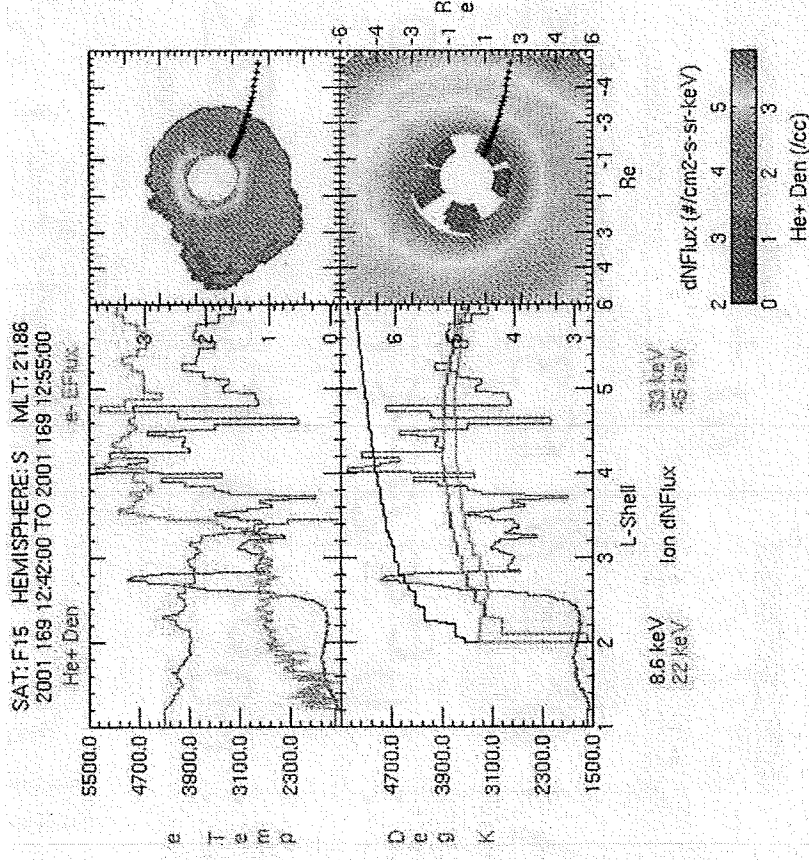
May 2-7, 1998: B-field Spectrogram (W/Ray),
and Electron Number Density Contours in $\log(\text{cm}^{-3})$



May 2-7, 1998 Magnetic Storm
Electron Thermal Fluxes due to EMIC Waves



Ionospheric Heating and EMIC Waves



After Gurgiolo *et al.*, JGR, 2005:

- Outer heating events occur within 0.75Re of the plasmapause in the evening MLT sector.
- Landau damping of the EMIC waves is a likely candidate to drive the heat flux into the ionosphere.
- Where are the precipitating ions which should accompany the EMIC wave instability in the outer heating events?

PA Diffusion Coefficient: Model Calculations

$$B^2(\omega) \approx \exp \left\{ -\frac{(\omega - \omega_m)^2}{\delta\omega^2} \right\}, \omega_{LC} \leq \omega \leq \omega_{UC},$$

$$\omega_{LC} = \omega_m - \delta\omega, \omega_{UC} = \omega_m + \delta\omega, \omega_m = 3\Omega_{O^+}, \delta\omega = 0.5\Omega_{O^+}$$

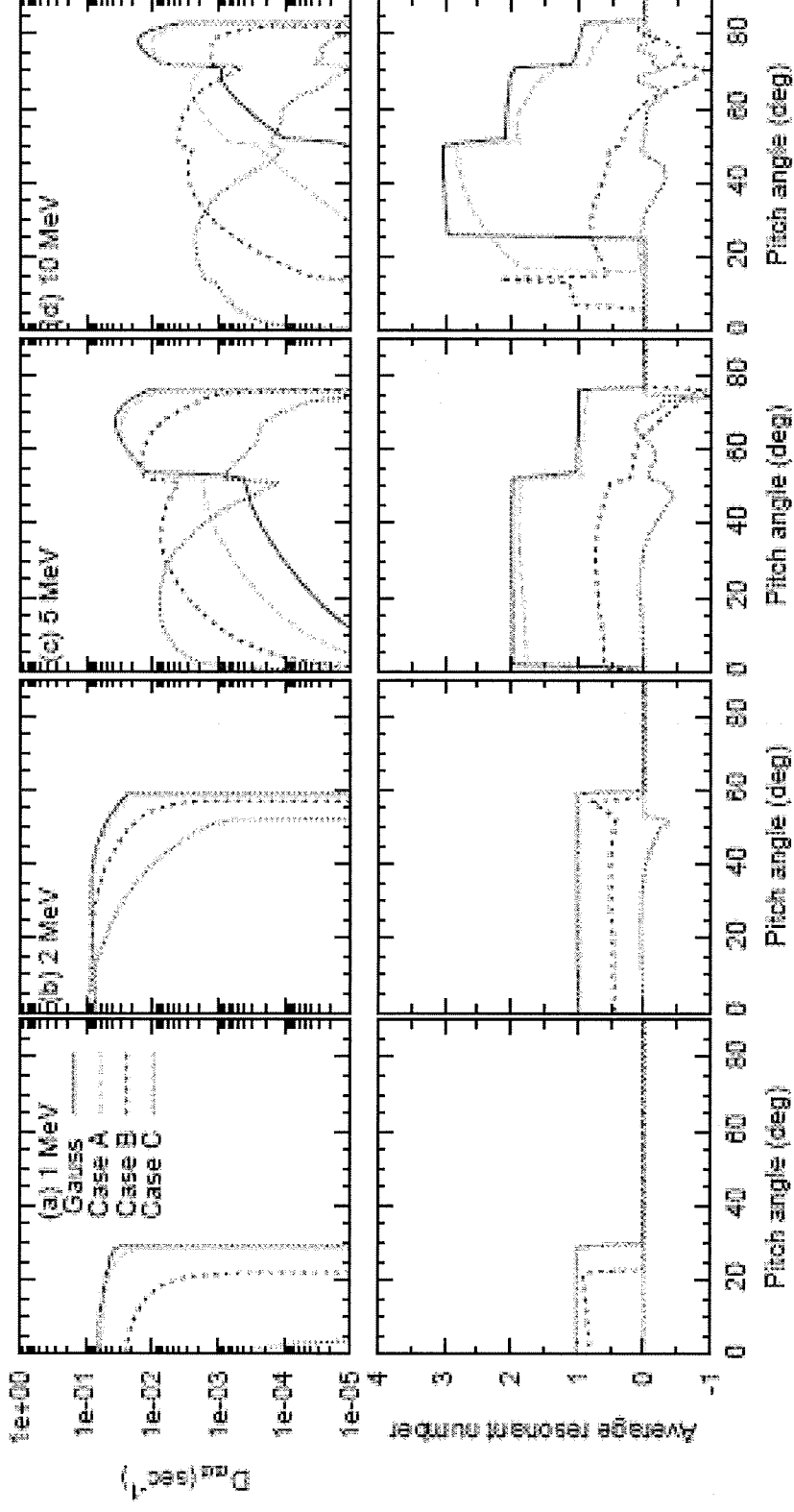
$$\text{Case A: } 0^\circ \leq \theta \leq 30^\circ, 150^\circ \leq \theta \leq 180^\circ$$

$$\text{Case B: } 30^\circ \leq \theta \leq 60^\circ, 120^\circ \leq \theta \leq 150^\circ$$

$$\text{Case C: } 60^\circ \leq \theta \leq 89^\circ, 91^\circ \leq \theta \leq 120^\circ$$

$$\iint B^2(\omega, \theta) d\omega d\theta = 1 \text{ nT}^2$$

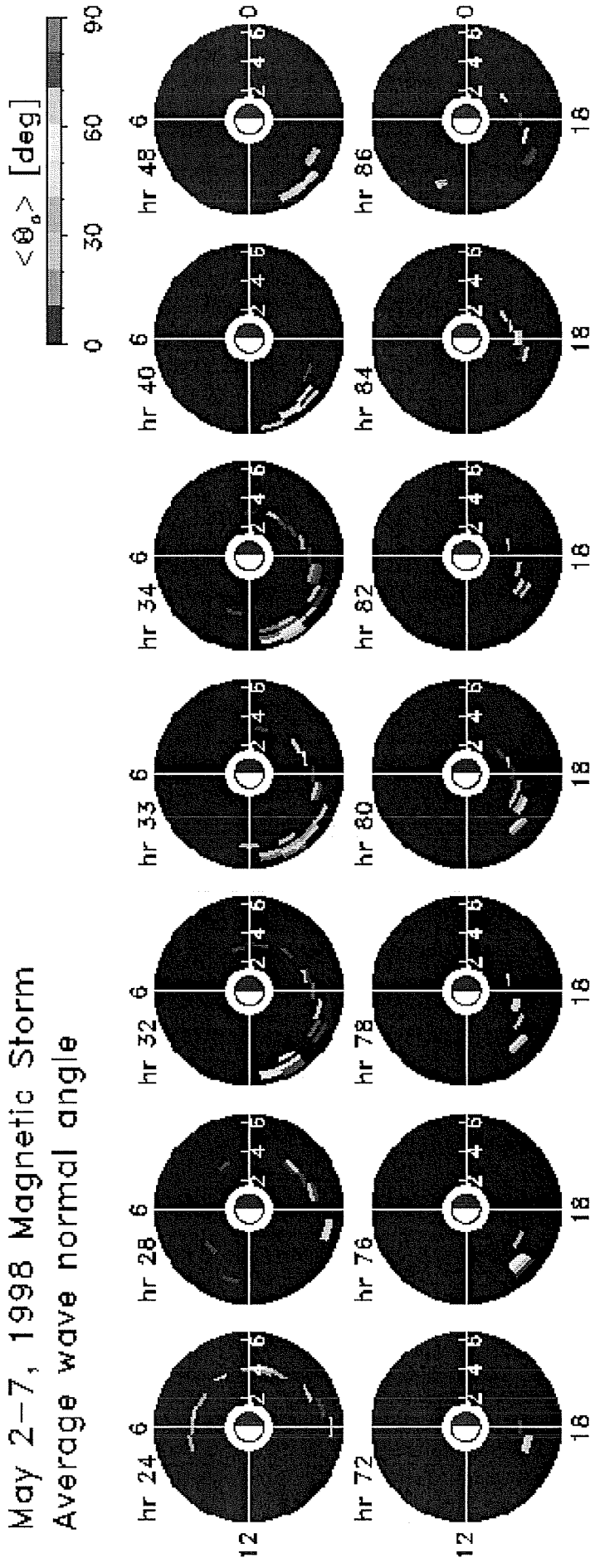
PA Diffusion Coefficient: Model Calculations



Equatorial electron diffusion by the He⁺-mode of EMIC waves. $L=4$, and $\left(\Omega_{pe}/\Omega_e\right)^2 = 10^3$. The curve “Gauss” is obtained for a wave normal angle distribution adopted by *Albert* [2003]. The second row shows the corresponding average resonant numbers.

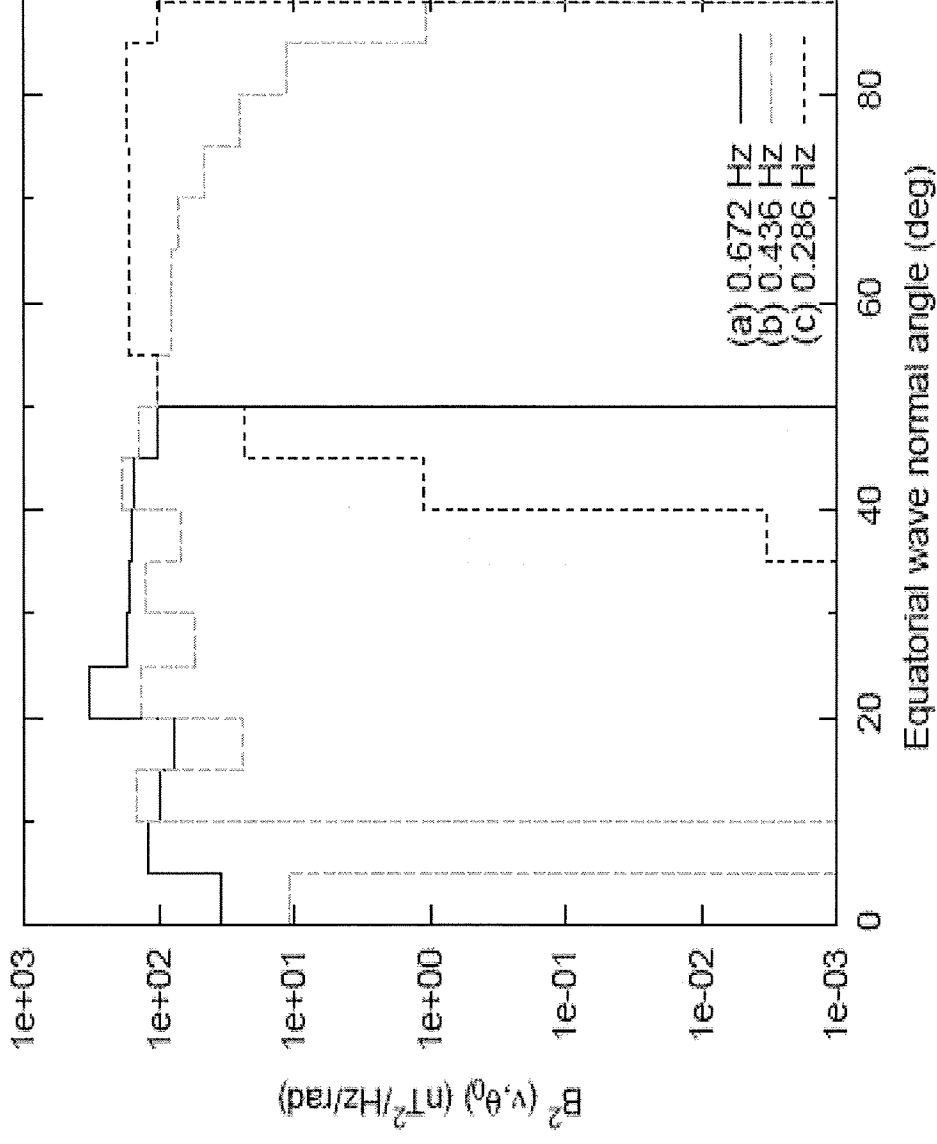
Average Equatorial WNA for He+-mode

May 2-7, 1998 Magnetic Storm
Average wave normal angle



The EMIC wave normal angle distributions are highly variable both in space and time, and the equatorial distributions range from a field-aligned distribution to a highly oblique distribution. The occurrences of the oblique and field-aligned wave normal angle distributions appear to be near the same during the May 1998 storm with a slight dominance of the former events.

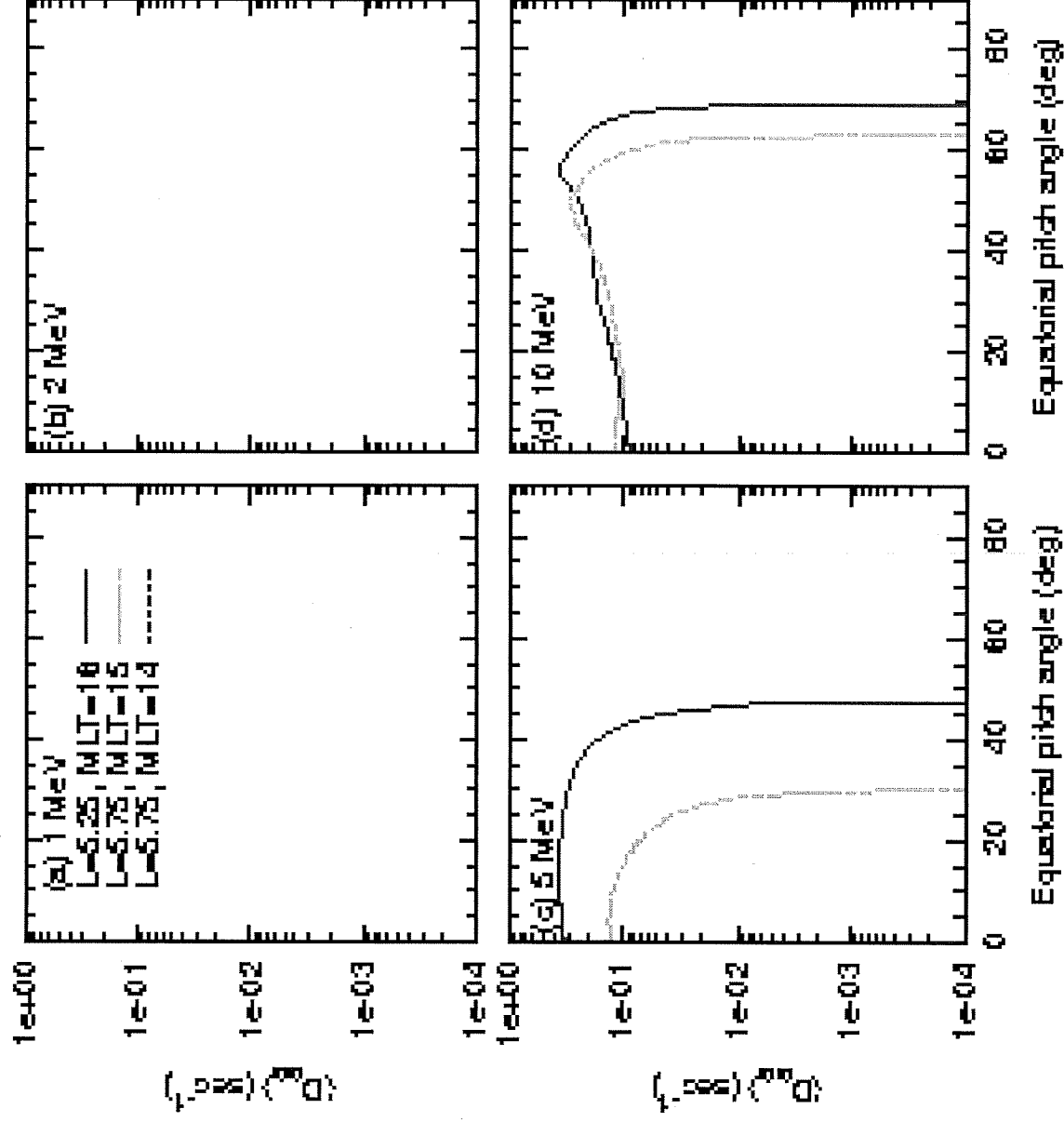
Equatorial PSD for He+-mode EMIC Waves



All the squared magnetic field spectra are obtained at 48 hours after 0000 UT on 1 May, 1998. (a) $L=5.25$, $MLT=16$, (b) $L=5.75$, $MLT=15$, and (c) $L=5.75$, $MLT=14$ [Khazanov *et al.*, 2006].

Only one model is capable to do this job. Convective growth rate is incapable to do this.

PA Diffusion Coefficients Based on the Normal Angle Distribution From the Model



SUMMARY

1. The SC RC Model with Propagating EMIC Waves in the Presence of Heavy Ions has been developed for the first time.
2. It is found that He⁺ mode energy distributions are not Gaussian distributions, and most important that wave energy can occupy not only the region of generation, i. e. the region of small wave normal angles, but occupies all wave normal angles, including those to near 90 degrees.
3. The latter is extremely crucial for RC precipitation, energy transfer to thermal plasmaspheric electrons by resonant Landau damping, and subsequent downward heat transport and excitation of stable auroral red arcs as well as for the scattering of relativistic electrons from outer RB.